UV-B Radiation-Induced Donor- and Acceptor-Side Modifications of Photosystem II in the Cyanobacterium *Synechocystis* sp. PCC 6803†

Imre Vass,*,‡,§ Diana Kirilovsky,‡ and Anne-Lise Etienne‡

Laboratoire de Photorégulation et Dynamique des Membranes Végétales, URA 1810 CNRS, Ecole Normale Supérieure, 46 rue d'Ulm, 75230 Paris Cedex 05, France, and Institute of Plant Biology, Biological Research Center of the Hungarian Academy of Sciences, P.O. Box 521, H-6701 Szeged, Hungary

Received May 13, 1999; Revised Manuscript Received July 15, 1999

ABSTRACT: We studied the effect of UV-B radiation (280−320 nm) on the donor- and acceptor-side components of photosystem II in the cyanobacterium *Synechocystis* sp. PCC 6803 by measuring the relaxation of flash-induced variable chlorophyll fluorescence. UV-B irradiation increases the $t_{1/2}$ of the decay components assigned to reoxidation of Q_A^- by Q_B from 220 to 330 μs in centers which have the Q_B site occupied, and from 3 to 6 ms in centers with the Q_B site empty. In contrast, the $t_{1/2}$ of the slow component arising from recombination of the $Q_AQ_B^-$ state with the S_2 state of the water-oxidizing complex decreases from 13 to 1−2 s. In the presence of DCMU, fluorescence relaxation in nonirradiated cells is dominated by a 0.5−0.6 s component, which reflects Q_A^- recombination with the S_2 state. After UV-B irradiation, this is partially replaced by much faster components ($t_{1/2} \approx 800-900$ μs and 8−10 ms) arising from recombination of Q_A^- with stabilized intermediate photosystem II donors, $P680^+$ and Tyr-Z^+. Measurement of fluorescence relaxation in the presence of different concentrations of DCMU revealed a 4−6-fold increase in the half-inhibitory concentration for electron transfer from Q_A to Q_B. UV-B irradiation in the presence of DCMU reduces Q_A in the majority (60%) of centers, but does not enhance the extent of UV-B damage beyond the level seen in the absence of DCMU, when Q_A is mostly oxidized. Illumination with white light during UV-B treatment retards the inactivation of PSII. However, this ameliorating effect is not observed if de novo protein synthesis is blocked by lincomycin. We conclude that in intact cyanobacterium cells UV-B light impairs electron transfer from the Mn cluster of water oxidation to Tyr-Z^+ and $P680^+$ in the same way that has been observed in isolated systems. The donor-side damage of PSII is accompanied by a modification of the Q_B site, which affects the binding of plastoquinone and electron transport inhibitors, but is not related to the presence of Q_A^-. White light, at the intensity applied for culturing the cells, provides protection against UV-B-induced damage by enhancing protein synthesis-dependent repair of PSII.

UV-B (280−320 nm) radiation is an important damaging factor of the photosyntetic apparatus, with its most sensitive target being the light energy-converting photosystem II (PSII)[1] complex (*1*, *2*). PSII is a water/plastoquinone oxidoreductase embedded in the thylakoid membrane, which transfers the electrons liberated from light-induced oxidation of water to membrane soluble plastoquinone molecules (for a review, see ref *3*). The redox cofactors of PSII electron transport are bound to or contained by the D1 and D2 protein subunits which form the reaction center of PSII (*4*). Water oxidation is catalyzed by a Mn cluster, and electrons liberated during this process are transferred to the reaction center chlorophyll, P680, via a redox active tyrosine residue, Tyr-Z, of the D1 protein. On the acceptor side of PSII, the electron produced by the light-induced charge separation event reduces a pheophytin molecule and then the first, Q_A, and second, Q_B, plastoquinone electron acceptors. Q_A is a firmly bound component of the reaction center complex, which undergoes one-electron reduction. In contrast, Q_B is a mobile electron carrier, which takes up two electrons sequentially from Q_A before leaving its binding site formed by the D1 protein. The side product of PSII function is molecular oxygen, which has been the source of atmospheric oxygen during the course of evolution, and hence is the origin of the UV-B screening ozone veil that protects life on Earth.

The mechanism of damage induced by UV-B light to the electron transport and protein structure of PSII has been addressed by a number of studies mostly in in vitro systems. According to a widely accepted view, in isolated PSII preparations the primary UV damage occurs at the donor side, most likely at the Mn cluster of water oxidation (*5*−*8*). However, UV-B-induced modification or loss of the function of the Q_A and Q_B quinone electron acceptors (*7*, *9*−*11*) and the Tyr-D and Tyr-Z donors (*7*, *12*) has also been

† The work was supported by grants from EU (ENV4-CT07-0493), INCO-Copernicus (ERB IC15-CT98-0126), the Hungarian National Committee for Technological Development OMFB (01800/98), and the Hungarian Scientific Research Fund, OTKA (T 030592).

* To whom correspondence should be addressed: Institute of Plant Biology, Biological Research Center of the Hungarian Academy of Sciences, P.O. Box 521, H-6701 Szeged, Hungary. Phone: +36-62-432-232. Fax: +36-62-433-434. E-mail: imre@nucleus.szbk.u-szeged.hu.

‡ Loboratoire de Photorégulation et Dynamique des Membranes Végétales.

§ Hungarian Academy of Sciences.

[1] Abbreviations: DCMU, 3-(3,4-dichlorophenyl)-1,1-dimethylurea; PSII, photosystem II; PQ, plastoquinone.

10.1021/bi991094w CCC: $18.00
Published on Web 09/03/1999

observed. Besides the electron transport components, UV-B light also damages the D1 and D2 reaction center subunits of PSII, leading eventually to their degradation (*9*, *10*, *13*−*16*). A further consequence of UV-B exposure of isolated systems is an apparent resistance against electron transport inhibitors, which act by replacing the mobile plastoquinone electron acceptor at its binding site formed by the D1 protein. This effect, which is most likely related to the UV-B-induced modification of the Q_B/herbicide binding site, has been observed in isolated thylakoids and BBY membranes (*5*, *6*), as well as in isolated reaction centers of the purple bacterium *Rhodobacter sphaeroides* (*17*), which have reaction center subunits and quinone acceptors analogous to those of PSII.

Although there are experimental observations which indicate that UV-B radiation induces donor-side damage in PSII in vivo (*1*, *18*), no unambiguous proof for this hypothesis has been provided yet. There is also a gap in our knowledge concerning the existence and importance of UV-B-induced acceptor-side modifications in vivo. A further point of interest is clarifying the putative role of Q_A^- in mediating UV-B damage in PSII in vivo (*19*, *20*). A useful, noninvasive method of following both donor- and acceptor-side events of PSII in intact photosynthetic organisms is monitoring the relaxation of the flash-induced increase in variable chlorophyll fluorescence yield. This process reflects the reoxidation of Q_A^- via forward electron transport to Q_B (and Q_B^-) and back reactions with donor-side components (*21*, *22*). By utilizing recent technical developments, it is possible to measure the relaxation of the variable fluorescence yield in the wide time range of 100 μs to 100 s after single-flash excitation (*23*) and obtain simultaneous information for donor- and acceptor-side modifications.

In this work, the UV-B effect was studied in the cyanobacterium *Synechocystis* sp. PCC 6803. We provide data supporting the idea that UV-B light damages the PSII donor side not only in vitro but also in vivo. In addition to the donor-side effect, UV-B light induces a modification of PQ and inhibitor binding to the Q_B pocket. However, the presence of Q_A^- during UV-B exposure does not affect the extent of UV-induced damage.

MATERIALS AND METHODS

Culture Conditions. Synechocystis sp. PCC 6803 cells were routinely grown in the mineral medium as described previously (*24*) in a rotary shaker at 30 °C under a 5% CO_2-enriched atmosphere. The intensity of white light during growth was 90 μE m^{-2} s^{-1}. Cells in the exponential growth phase (A_{580} of 0.6−0.8) were harvested by centrifugation for 10 min at 4000*g* at room temperature and resuspended at a concentration of 10 μg of Chl *a*/mL in fresh culture medium containing 50 mM HEPES (pH 6.8).

UV-B Treatment. UV-B irradiation was performed in open, cylindrical glass containers in which the cell suspension formed a 45 mm high layer, with continuous stirring at room temperature. A Vilbert-Lourmat VL-215M lamp was used as the UV-B light source, with maximal emission at 312 nm, in combination with eight layers of 0.1 mm cellulose acetate filters (Clarfoil, Courtaluds Chemicals) to screen out any UV-C contribution. The spectral distribution of the UV lamp is shown in our previous publication (*25*). Under these conditions, the UV-B intensity was 2.4 W m^{-2} (≈6.3 μE m^{-2} s^{-1}) at the surface of the cell suspension as measured with a Cole-Parmer radiometer (model 97503-00) equipped with a 312 nm sensor. Due to the high optical density of the cell suspension, the average UV-B irradiation intensity was only approximately 0.09 W m^{-2} (≈0.24 μE m^{-2} s^{-1}) within the cell suspension, calculated by taking into account the absorption by the optically dense sample according to ref *26*. In some experiments, the cell suspension was illuminated with 120 μE m^{-2} s^{-1} white light during the course of UV-B irradiation. For monitoring the recovery process, the UV-B-irradiated cells were transferred back to the growth chamber where they were exposed to normal culture conditions.

Fluorescence Relaxation Kinetics. Flash-induced increases and the subsequent decay of chlorophyll fluorescence yield was measured by a double-modulation fluorometer (PSI Instruments, Brno) (*23*). The instrument contained red LEDs for both actinic (20 μs) and measuring (2.5 μs) flashes, and was used in the 100 μs to 100 s time range with cells diluted to a concentration of 2 μg of Chl/mL. With this type of measurement, it is crucial to avoid distortion of the relaxation kinetics due to the actinic effect of measuring flashes. This was carefully checked, and the intensity of the measuring flashes was set at a value that was low enough to avoid reduction of Q_A in the presence of DCMU.

Analysis of the fluorescence relaxation kinetics was based on the widely used model of the two-electron gate (*21*, *27*). According to this model, the fast (few hundred microseconds) decay component reflects Q_A^- reoxidation via forward electron transport in centers which contain bound PQ (in the oxidized or semireduced form) at the Q_B site before the flash. The middle (few milliseconds) phase arises from Q_A^- reoxidation in centers which had an empty Q_B site at the time of the flash and have to bind a PQ molecule from the PQ pool. Finally, the slow (few seconds) phase reflects Q_A^- reoxidation via back reaction with the S_2 state of the water-oxidizing complex. The fast and middle phases are generally described by exponential components. In contrast, the slow decay of Q_A^- via charge recombination has been shown to obey hyperbolic decay kinetics corresponding to an apparent second-order process (*28*). Consequently, multicomponent deconvolution of the measured curves was performed by using a fitting function with two exponential components and one hyperbolic component:

$$F(t) - F_o = A_1 \exp(-t/T_1) + A_2 \exp(-t/T_2) + A_3/(1 + t/T_3)$$

where $F(t)$ is the variable fluorescence yield, F_o is the basic fluorescence level before the flash, A_1−A_3 are the amplitudes, T_1−T_3 are the time constants from which the half-lifetimes can be calculated via $t_{1/2} = \ln 2\ T$ for the exponential components, and $t_{1/2}$ is the T for the hyperbolic component.

Variable Chlorophyll Fluorescence Measurements. Steady-sate variable fluorescence was measured by a PAM machine (WALZ, Effeltrich, Germany), using a home-built computer-controlled data acquisition system.

Oxygen Evolution Measurements. Steady-state rates of oxygen evolution were measured using a Hansatech DW2 O_2 electrode at a light intensity of 1000 μE m^{-2} s^{-1} in the presence of 0.5 mM 2,5-dimethyl-*p*-benzoquinone as an

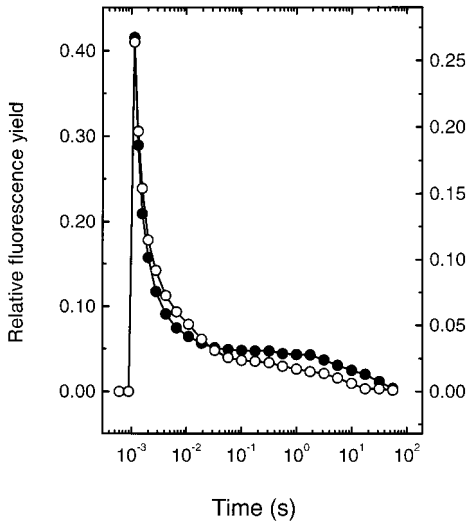

FIGURE 1: Effect of UV-B irradiation on the fluorescence relaxation of *Synechocystis* sp. PCC 6803. Cells were exposed to UV-B irradiation for 0 (white symbols) and 45 min (black symbols) in the presence of 100 μg/mL lincomycin. Relaxation of the flash-induced chlorophyll fluorescence yield was measured without addition. The curves are normalized to the same amplitude, and the actual size of the signals is shown by the left (nonirradiated cells) and right scales (UV-B-irradiated cells).

electron acceptor. Typically, 2 mL of cells at a concentration of 10 μg of Chl *a*/mL was used in each measurement.

RESULTS

UV-B Effects on the Q_B Binding Pocket. In the nonirradiated control cells, the fluorescence yield relaxation is dominated by the fast (220 μs) phase, whose relative amplitude is about 70% (Figure 1). The contribution of the middle (3−4 ms) phase is 20%, and that of the slow phase (13 s) is about 10%. UV-B irradiation for 45 min in the presence of the protein synthesis inhibitor lincomycin, which prevents the repair of UV-induced protein damage to the D1 and D2 reaction center subunits, resulted in a 30−35% decrease in the total fluorescence amplitude (Figure 1), reflecting the loss of Q_A reduction that can be detected 100 μs after the flash. The UV-B treatment also affected the fluorescence yield relaxation kinetics by slowing the middle phase and accelerating the slow phase. This point was further investigated by measuring fluorescence decay in cells that were exposed to UV-B radiation for different periods of time. Analysis of these decay curves confirmed the gradual acceleration of the slow phase, from 13 to 1−2 s. In addition, the $t_{1/2}$ of the middle phase increased from 3 to 6 ms, and that of the fast phase from 220 to 330 μs (Table 1). The total fluorescence amplitude was decreased to 44% of its initial value by the end of the 90 min irradiation protocol. These data indicate modification of PQ binding at the Q_B site and/or a decrease in the apparent equilibrium constant for sharing the electron between Q_A and Q_B, as discussed below.

To determine if UV-B-induced modification of the Q_B site also affects binding of PSII electron transport inhibitors, inhibitor titration experiments were performed in cells which were irradiated UV-B light in the presence of the protein synthesis inhibitor lincomycin. The data summarized in Table 2 show the half-inhibitory concentrations of DCMU and metribuzin, calculated from the inhibitor titration curves of the slowly decaying (0.6 s) component, which reflects the amount of centers in which the $S_2Q_A^-$ recombination occurs. UV-B irradiation induced about 4- and 6-fold increases in the half-inhibitory concentrations of DCMU and metribuzin, respectively. The fluorescence results presented here were confirmed by inhibitor titration of oxygen evolution, which showed a 3-fold increase in of the pI_{50} value of DCMU. When UV-B irradiation was performed in the absence of lincomycin, allowing continuous protein repair, the increase in pI_{50} values was smaller, and this effect was reversible when the UV-B-irradiated cells were transferred to normal growth conditions under white light for 2−3 h (not shown).

UV-B Effects on the PSII Donor Side. When fluorescence relaxation is measured in the presence of DCMU, the decay has a sigmoidal shape when plotted on a logarithmic abscissa scale (Figure 2A). These curves are clearly not monoexponential; however, they can be satisfactorily fitted by using a single hyperbolic component yielding a half-lifetime of 0.6 s. A similar approach has been used by Bennoun for analysis of Q_A^- decay quantified from the complementary area above fluorescence induction curves in the presence of DCMU (*28*). After UV-B irradiation, the relaxation is considerably accelerated and a substantial fast decay is observed besides the slow component seen in the nonirradiated control cells (Figure 2A). Inhibitor titration of oxygen evolution in the same cells demonstrates that electron transport through PSII is completely inhibited at 30 μM DCMU (not shown), and thus, the Q_A to Q_B electron transfer step is fully blocked in the oxygen-evolving centers. In principle, the fast phase could arise from forward leak of electrons through the DCMU block in centers, which do not evolve oxygen. This possibility was explored by adding hydroxylamine and DCMU to the UV-irradiated cells. Hydroxylamine releases the Mn cluster from PSII (*29*), and it can reduce Tyr-Z^+ after its light-induced oxidation (*30*). Under these conditions, the electrons that are stabilized on Q_A^- by DCMU have no recombination partner. Accordingly, the flash-induced increase in fluorescence yield in the nonirradiated cells stays almost constant during the course of the measurement (Figure 2B). The same result was obtained in the UV-B-irradiated cells. Both the fast and slow decay phases seen in the presence of DCMU were eliminated by hydroxylamine (Figure 2B); i.e., the rapidly decaying phase should also arise from recombination reactions of Q_A^- with PSII donor-side component(s).

To check the validity of the above idea, *Synechocystis* cells were exposed to different periods of UV-B illumination and their fluorescence relaxation curves were measured in the presence of 30 μM DCMU. Satisfactory fitting of these decay curves required either two hyperbolic components with 2−3 ms and 0.6−0.8 s half-lifetimes or two exponential components ($t_{1/2}$ = 800 μs and 8−10 ms) and one hyperbolic component ($t_{1/2}$ = 0.6−0.8 s). The total fluorescence amplitude measured in the presence of DCMU is gradually decreased during UV-B illumination (Figure 3A), which is accompanied by a rapid loss of the slow decaying component and an increase in the fast decaying portion of the relaxation curves (Figure 3B). These changes in the decay amplitudes are completely reversed when cells are transferred to growth conditions under white light (Figure 3A,B). Treatment of the *Synechocystis* cells with the protein synthesis inhibitor lincomycin before UV-B irradiation accelerates the loss of

Table 1: Decay Kinetics of Flash-Induced Variable Fluorescence in *Synechocytis* sp. PCC 6803 Cells[a]

duration of UV-B irradiation (min)	total amplitude (%)	fast phase $t_{1/2}$ (μs) [amp (%)]	middle phase $t_{1/2}$ (ms) [amp (%)]	slow phase $t_{1/2}$ (s) [amp (%)]
		No Addition[b]		
0	100[d]	220 ± 20 (68 ± 3)[e]	2.9 ± 0.4 (23 ± 1.8)	13 ± 4 (9 ± 1.8)
20	83 ± 2	250 ± 25 (66 ± 2.7)	3.8 ± 0.5 (26 ± 1.9)	6.2 ± 3 (7 ± 1.4)
40	69 ± 2	300 ± 20 (68 ± 2.2)	5.6 ± 0.7 (26 ± 1.8)	3.1 ± 2 (6 ± 1.0)
60	61 ± 3	320 ± 24 (65 ± 2.5)	5.4 ± 0.7 (29 ± 2.0)	1.2 ± 0.8 (6 ± 0.9)
90	44 ± 2	330 ± 28 (68 ± 2.5)	5.9 ± 0.8 (26 ± 2.0)	2.2 ± 0.7 (6 ± 0.9)
		With DCMU[c]		
0	100	− (0)	2.1 ± 0.3 (3 ± 1.2)	0.59 ± 0.03 (97 ± 1.1)
20	85 ± 1	− (0)	2.7 ± 0.4 (27 ± 0.9)	0.69 ± 0.03 (73 ± 0.7)
40	69 ± 2	− (0)	2.7 ± 0.3 (37 ± 0.8)	0.86 ± 0.04 (63 ± 0.7)
60	58 ± 2	− (0)	2.4 ± 0.3 (43 ± 1.1)	0.83 ± 0.06 (57 ± 0.9)
90	46 ± 2	− (0)	2.6 ± 0.4 (43 ± 1.4)	0.81 ± 0.07 (57 ± 0.8)
		With DCMU[b]		
0	100	− (0)	2.1 ± 0.3 (3 ± 1)	0.59 ± 0.03 (97 ± 1.1)
20	85 ± 2	810 ± 60 (8 ± 3)	6.5 ± 0.3 (17 ± 3)	0.62 ± 0.02 (75 ± 0.9)
40	70 ± 1	780 ± 160 (17 ± 2)	10.2 ± 1.3 (21 ± 2)	0.78 ± 0.03 (62 ± 0.5)
60	59 ± 2	760 ± 130 (21 ± 2)	10.8 ± 1.4 (23 ± 2)	0.78 ± 0.03 (56 ± 0.7)
90	48 ± 2	800 ± 140 (21 ± 2)	11.1 ± 1.7 (24 ± 1.6)	0.78 ± 0.04 (55 ± 0.8)

[a] *Synechocystis* sp. PCC 6803 cells were irradiated with UV-B light for the indicated periods of time, and relaxation of the flash-induced fluorescence yield was measured with or without 30 μM DCMU. [b] The curves were analyzed in terms of two exponential components (fast and middle phases) and one hyperbolic component (slow phase). [c] The curves were analyzed in terms of two hyperbolic components (middle and slow phases). [d] Values represent the amplitude of total variable fluorescence as a percentage of that in the nonirradiated control. [e] Values in parentheses are relative amplitudes as a percentage of total variable fluorescence obtained after the given UV-B irradiation time. Standard errors of the calculated parameters are also indicated.

Table 2: Effect of UV-B Irradiation on the Half-Inhibitory Concentrations of DCMU and Metribuzin in *Synechocystis* sp. PCC 6803 Cells[a]

	[DCMU] (M)		[metribuzin] (M)	
	without UV-B	with UV-B	without UV-B	with UV-B
pI_{50}	4×10^{-7}	1.5×10^{-6}	2.5×10^{-6}	1.5×10^{-5}

[a] Cells were irradiated with UV-B light for 0 and 45 min in the presence of 100 μg/mL lincomycin. Relaxation of flash-induced variable fluorescence yield was measured after addition of various concentrations of DCMU and metribuzin as described in the legend of Figure 1, and the curves were analyzed by using two exponential components and one hyperbolic decay component. The amplitude of the slow decaying hyperbolic component, which reflects the recombination of Q_A^- with the S_2 state, was plotted as a function of herbicide concentration, and the half-inhibitory concentrations were determined.

total fluorescence amplitude and of the slow phase, whereas it induces a more rapid formation of the fast decay (Figure 3A,B). Lincomycin also blocks the recovery of both the total variable fluorescence, as well as the changes in the amplitudes of the fast and slow decaying phases.

Effect of Visible Light on UV-B-Induced Damage. The interaction of visible and UV-B light is a very important issue since under natural conditions plants are exposed simultaneously to these spectral ranges of sunlight. One possible effect of illumination with white light can be the formation of reduced Q_A, which has previously been suggested to be a potential UV-B target (*19*). To explore this possibility, we determined the redox state of Q_A under illumination with UV-B light, and UV-B and white light. In the absence of DCMU, UV-B radiation alone or in combination with 120 μE m^{-2} s^{-1} white light induced only a small extent (approximately 10%) of Q_A reduction (Figure 4, curve a). It is noteworthy, however, that both illumination protocols induced an about 40% increase in the F_{max} level, measured with saturating pulses of white light, which effect is most likely related to the increase in fluorescence yield due to induction of the state II-to-state I transition (*31*). Unexpectedly, the 6.3 μE m^{-2} s^{-1} UV-B radiation alone could reduce Q_A in ≈60% of the centers in the presence of 30 μM DCMU, whereas 120 μE m^{-2} s^{-1} white light resulted in Q_A reduction in about 65% of the centers. The combination of the UV-B and white light closed about 80% of the centers in the presence of DCMU (Figure 4, curve b).

When UV-B irradiation was performed in the presence of DCMU, the total fluorescence amplitude exhibited the same extent of loss that was observed with UV-B alone (Figure 5A), although the reduction level of Q_A was much higher in the presence than in the absence of DCMU (Figure 4). The changes in the relative amplitudes of the fast and slow decay phases of fluorescence relaxation followed also the same kinetics in the presence and absence of DCMU (Figure 5B). Interestingly, when background illumination with white light was applied during the course of UV-B irradiation, a very clear ameliorating effect was observed. This is shown by the considerably retarded decrease in the amplitude of the total fluorescence and that of the slow phase (panels A and B of Figure 5, respectively), as well as by the retarded increase in the amplitude of the fast recombination phase (Figure 5B).

The above results show that the increased reduction level of Q_A does not accelerate UV-B-induced damage of PSII. On the other hand, the presence of white light decreases the extent of UV-B-induced damage. Previous results have demonstrated that de novo synthesis of the D1 and D2 reaction center subunits plays an important role in the restoration of UV-B-damaged PSII activity (*32*, *33*). Consequently, the favorable effect of white illumination is possibly related to enhanced protein synthesis. This idea is fully confirmed by the data depicted in Figure 6, where the effect of UV-B radiation on the inhibition of oxygen evolution was followed. UV-B-induced inhibition of oxygen

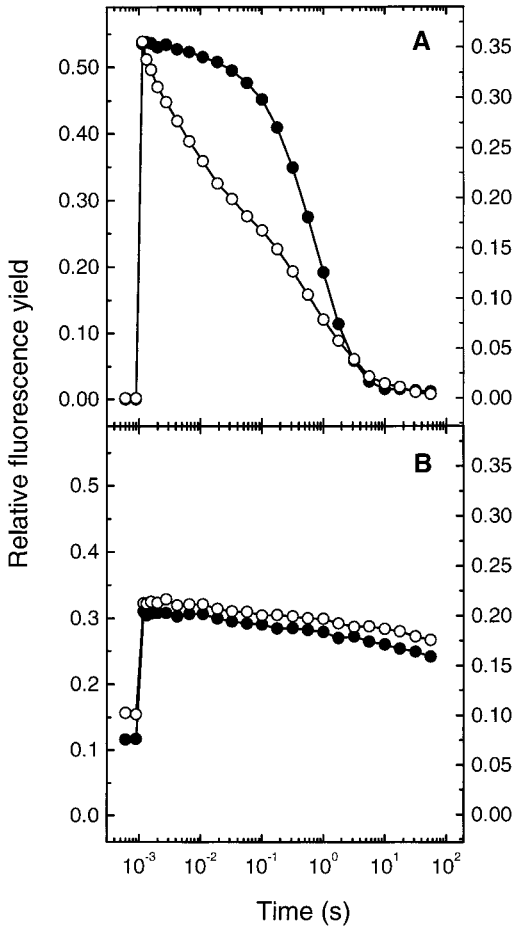

FIGURE 2: Effect of UV-B irradiation on the fluorescence relaxation of *Synechocystis* sp. PCC 6803 in the presence of DCMU. Cells were exposed to UV-B irradiation for 0 (black symbols) and 45 min (white symbols) in the presence of 100 μg/mL lincomycin. Relaxation of the flash-induced chlorophyll fluorescence yield was measured in the presence of 30 μM DCMU (A) and in the presence of 30 μM DCMU and 5 mM hydroxylamine (B). The curves are normalized in the same way as in Figure 1.

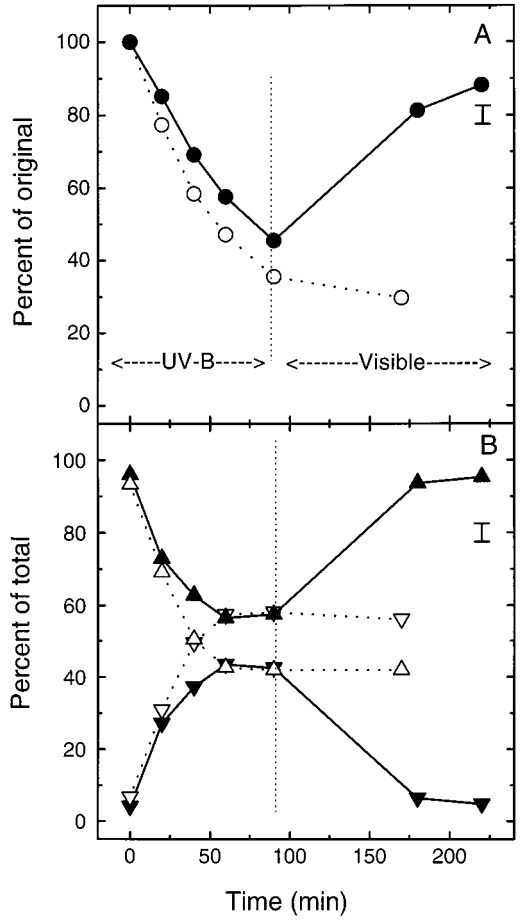

FIGURE 3: UV-B-induced loss and subsequent recovery of flash-induced chlorophyll fluorescence yield in *Synechocystis* sp. PCC 6803. Cells were exposed to UV-B radiation for 90 min and then transferred to visible light. Flash-induced fluorescence was measured in the presence of 30 μM DCMU and analyzed in terms of two hyperbolic components, or two exponential components and one hyperbolic component, as in Table 1. (A) Total fluorescence amplitude without addition (●) and in the presence of 100 μg/mL lincomycin (○). (B) The relative amplitudes of the slow hyperbolic phase (up triangles) as well as of the fast phase, represented by the amplitude of the fast hyperbolic component, which is the same as the sum of the two exponential components (down triangles), are expressed as a percentage of the total fluorescence amplitude at the given time. The black and white symbols represent results obtained in the absence and presence of 100 μg/mL lincomycin, respectively. The error bars show the typical standard error of the plotted data.

evolving activity is slowed when illumination with white light is applied together with UV-B light. Importantly, this beneficial effect is completely canceled by lincomycin, and the inhibition of oxygen evolution follows the same course that was observed under UV-B irradiation alone in the presence of lincomycin (Figure 6).

DISCUSSION

In this work, we studied the effects of UV-B irradiation on the characteristics of donor- and acceptor-side electron transport in *Synechocystis* sp. PCC 6803 cells. The main method of investigation was the measurement of fluorescence yield relaxation following a single saturating flash. By using the double-modulation technique (*23*), we could measure fluorescence yield changes in a very broad time range, from 100 μs to 100 s, and study reoxidation processes of Q_A^- by both forward and back reactions. A surprising result from these measurements was that the decay kinetics in the presence of DCMU are clearly not monoexponential, as could be expected for the $S_2Q_A^-$ recombination, but can be fitted well with a single hyperbolic component. Hyperbolic decay of Q_A^- via charge recombination, which would imply second-order kinetics for the recombination process, has been proposed earlier by Bennoun (*28*). Our own experience also shows that in *Synechocystis* sp. PCC 6803 cells the thermoluminescence component which arises from the recombination of $S_2Q_A^-$ cannot be described by first-order kinetics; instead, a theoretical model with apparent second-order kinetics is needed (I. Vass et al., unpublished results). However, the mechanistic background for this phenomenon is not well-understood. The data of Bennoun show that the rate constant of the decay does not depend on the amount of Q_A^-; thus, it does not reflect a true bimolecular mechanism (*28*). Hyperbolic decay kinetics of $S_2Q_A^-$ recombination have also been observed by Lavorel et al. using delayed luminescence, which was proposed to reflect a distribution of first-order charge recombination rate constants over PSII centers in which the mutual orientations and distances of the redox cofactors and/or the conformation of the reaction center is not completely identical due to differences in the membrane environment (*44*).

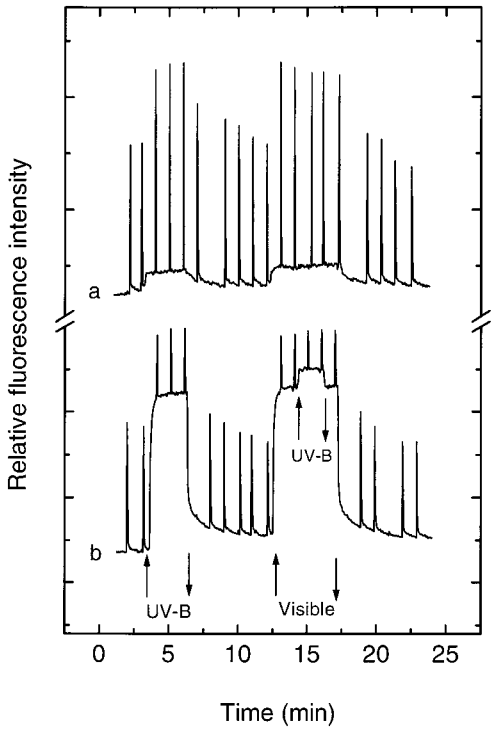

FIGURE 4: Reduction of Q_A under UV-B and white light illumination in *Synechocystis* sp. PCC 6803. The level of steady-state fluorescence reflecting the extent of Q_A reduction was monitored by using the weak measuring light of the PAM fluorimeter. The maximal fluorescence, representing full reduction of Q_A, was induced by 500 ms saturating light pulses. At the times denoted by arrows, UV-B light (6.3 μE m^{-2} s^{-1}) and continuous white light (120 μE m^{-2} s^{-1}) were switched on and off. The measurements were performed in the absence (curve a) and in the presence of 30 μM DCMU (curve b).

UV-B Effects on the Q_B Binding Pocket. Analysis of fluorescence relaxation traces in UV-B-irradiated *Synechocystis* cells revealed modifications of the Q_B niche which affect the binding of both PQ and electron transport inhibitors. In the nonirradiated cells, the slow phase of decay has a half-lifetime of about 12−13 s, which is decreased to 0.6−0.8 s in the presence of DCMU. Since the slow phase should reflect the reoxidation of Q_A^- via charge recombination with the S_2 state in both cases, the differences in the half-lifetimes indicate that in the absence of DCMU the recombination occurs from the $Q_AQ_B^-$ state, which is in charge equilibrium with $Q_A^-Q_B$. The relationship of recombination half-lifetimes occurring through charge equilibrium can be described as

$$t_{1/2}(S_2Q_AQ_B^-) = t_{1/2}(S_2Q_A^-) \times (1 + K_{app})$$

where K_{app} is the apparent equilibrium constant for sharing the electron between Q_A and Q_B (*34*). Using a $t_{1/2}(S_2Q_AQ_B^-)$ of 12−13 s and a $t_{1/2}(S_2Q_A^-)$ of 0.6−0.8 s, K_{app} is approximately 16. This approximation agrees well with previous reports of K_{app} being 15−20 (*35*, *36*), which provides firm support for the analysis of fluorescence relaxation curves presented here.

Since in the UV-B-irradiated cells the half-lifetime of the slow phase is decreased in the absence ($S_2Q_AQ_B^-$ recombination), but not in the presence ($S_2Q_A^-$ recombination) of DCMU (Table 1), K_{app} should be decreased. This effect might be caused by an energetic change in Q_B^- stability, or related to a decreased affinity of PQ binding. The latter possibility

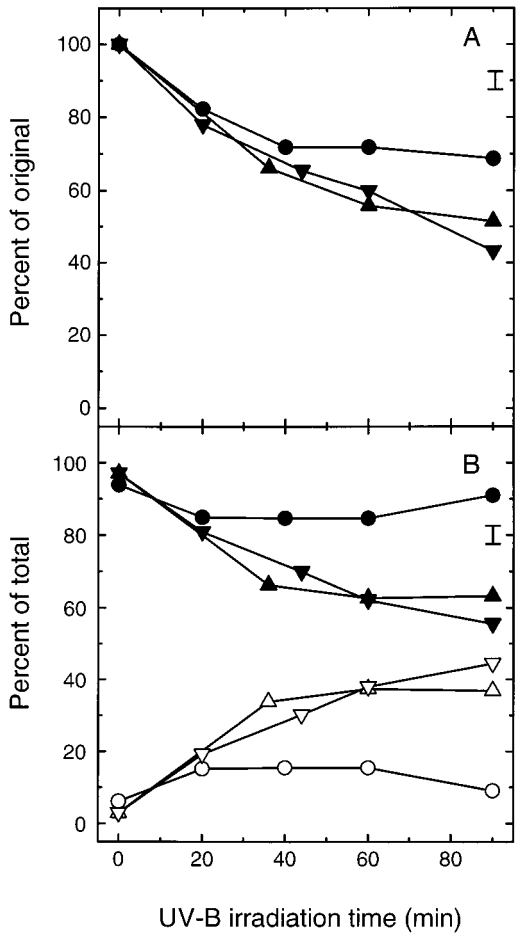

FIGURE 5: Effect of white light and DCMU on the UV-B-induced modification of fluorescence relaxation in *Synchecocystis* sp. PCC 6803. Cells were exposed to UV-B light without addition (up triangles) and after addition of 30 μM DCMU (down triangles) and in the presence of 120 μE m^{-2} s^{-1} white light (circles). Flash-induced fluorescence was measured in the presence of 30 μM DCMU and analyzed as described in the legend of Figure 3. Panel A shows the changes in the total fluorescence amplitude expressed as a percentage of its value in the nonirradiated control. Panel B shows the changes in the relative amplitudes of the fast (white symbols) and slow recombination components (black symbols) expressed as a percentage of the total fluorescence amplitude at a given time. The error bars show the typical standard error of the plotted data.

is indicated by the increase in the $t_{1/2}$ of the middle phase from 3 to 6 ms (Table 1). This decay component is assigned to reoxidation of Q_A^- in centers in which a vacant Q_B site has to be reoccupied by a PQ molecule before the Q_A^- to Q_B electron transfer can take place. Thus, the increase in its $t_{1/2}$ is consistent with a slower PQ binding in the UV-B-irradiated cells. The small increase observed in the $t_{1/2}$ of the fast phase (Table 1) indicates a slower electron transfer from Q_A^- to bound Q_B, which is possibly also the consequence of the Q_B site modification.

A further manifestation of the UV-B-induced change in the Q_B/herbicide binding niche is the 4−6-fold increase in the pI_{50} values of DCMU and metribuzin (Table 2). These results are in a good agreement with previous observations with isolated thylakoids (*5*, *6*, *37*) and purple bacterial reaction centers (*17*), and demonstrate that UV-B irradiation leads to a decreased affinity of herbicide binding in intact cells, too.

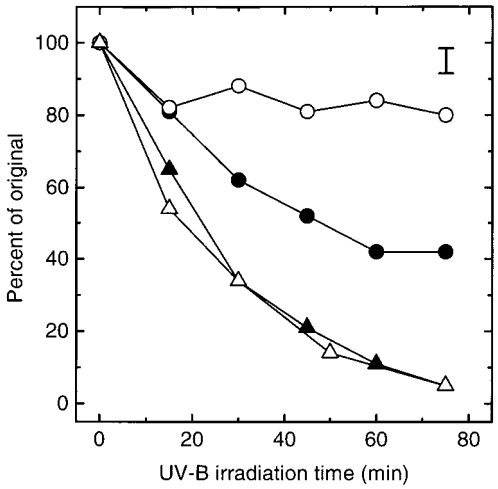

FIGURE 6: Effect of white light and lincomycin on the UV-B-induced inhibition of oxygen evolution in *Synechecocystis* sp. PCC 6803. Cells were exposed to UV-B light, and the rate of oxygen evolution is plotted as a function of irradiation time. UV-B irradiation was performed without addition (●), in the presence of 100 μg/mL lincomycin (▲), in the presence of background illumination with 120 μE m^{-2} s^{-1} white light (○), and in the presence of 120 μE m^{-2} s^{-1} white light and 100 μg/mL lincomycin (△). The error bar shows the typical standard error of the plotted data.

UV-B Effects on the PSII Donor Side. The kinetics of fluorescence yield relaxation exhibit a dramatic acceleration when measured in UV-B-irradiated cells in the presence of high concentrations of DCMU (Figure 3A) or metribuzin (not shown). This effect shows the existence of heterogeneous recombination reactions of Q_A^- with donor-side components in UV-damaged PSII. The slow component ($t_{1/2}$ = 0.6−0.8 s) arises from the $S_2Q_A^-$ recombination in centers that retain intact Mn cluster. A likely candidate for the recombination partner being involved in the fast component is Tyr-Z^+, which is stabilized in centers in which electron transfer from the Mn cluster is inhibited by UV-B. This hypothesis is fully supported by the observations of Chu et al. (*38*), who have shown that fluorescence decay in the presence of DCMU is accelerated in *Synechocystis* sp. PCC 6803 mutants which lack a functional Mn cluster. These authors assigned the fast fluorescence decay, fitted with an exponential component with $t_{1/2}$ varying between 3.5 and 50 ms, to the recombination of Q_A^- and Tyr-Z^+. In our case, the fast decay could not be fitted with one exponential component. Assuming that hyperbolic fluorescence decay kinetics are characteristic of recombination reactions, we used a hyperbolic component to describe the fast decaying part of relaxation curves measured in the presence of fully inhibiting DCMU in UV-B-treated cells, which yielded a satisfactory fit with a half-lifetime of 2−3 ms. Since this value appeared to be too fast for the Q_A^-Tyr-Z^+ recombination (*38*), the curves were also analyzed by using two exponential components for the fast decaying phase. This approach resulted in 800 μs and 8−10 ms half-lifetimes. The faster component could correspond to the about 1 ms recombination time of $P_{680}^+Q_A^-$ observed in isolated core particles of *Synechocystis* sp. PCC 6803 (*39*). The longer half-lifetime is within the range that was observed for Tyr-$Z^+Q_A^-$ recombination in intact cells that lack a functional Mn cluster (*38*). Since recombination of Tyr-Z^+ with Q_A^- proceeds via the Tyr-$Z^+P_{680}Q_A^-$ ↔ Tyr-$ZP_{680}^+Q_A^-$ charge equilibrium, their $t_{1/2}$ values are correlated according to the formula

$$t_{1/2}(\text{Tyr-}Z^+Q_A^-) = t_{1/2}(P_{680}^+Q_A^-) \times (1 + K_{app,ZP})$$

where $K_{app,ZP}$ is the apparent equilibrium constant for sharing an electron between Tyr-Z and P_{680}. From our data, $K_{app,ZP}$ would be 13−14 in the UV-B-inhibited PSII centers. From this consideration, it also follows that the amplitude of the 800 μs phase should be only a $1/K_{app,ZP}$ (0.07−0.08) fraction of the amplitude of the 8−10 ms phase if the recombination proceeds via the Z^+P_{680} ↔ Tyr-ZP_{680}^+ equilibrium in all centers. In contrast to this expectation, the results of the fit give about 70−80% for the amplitude of the 800 μs phase compared to that of the 8−10 ms phase (Table 1). A straightforward explanation for this phenomenon would be to assume that with the progress of UV-B exposure not only the Mn cluster but also Tyr-Z is damaged, and most of the 800 μs phase arises from centers where the Tyr-Z to P_{680}^+ electron transfer step is impaired. This idea is in agreement with our earlier in vitro study which showed that the inactivation of the Mn cluster is followed by a slower inactivation of Tyr-Z function (*7*).

Although from the available data it cannot be unambiguously determined if the fast decaying fluorescence component observed in the presence of DCMU in the UV-B-irradiated cells represents a single hyperbolic phase or two exponential phases, we prefer the second option. In both cases, however, the 2−3 and 8−10 ms half-lifetimes assigned to the Tyr-$Z^+Q_A^-$ recombination obtained from the hyperbolic and exponential fitting, respectively, are at the lower end of the 3.5−50 ms range reported by Chu et al. (*38*) for different mutants that lack the functional Mn cluster. The variation in $t_{1/2}$ in those mutants was explained by a modification of the redox potential of Tyr-Z. Since in isolated core particles of wild-type cells (*39*) the Tyr-$Z^+Q_A^-$ recombination has an 80 ms time constant, it is likely that UV-B irradiation decreases the redox potential of Tyr-Z as a consequence of inactivating the Mn cluster, or due to a structural change in the PSII reaction center.

It follows from the above interpretation that the appearance of the fast decay of fluorescence relaxation in the presence of DCMU reflects charge recombination between Tyr-Z^+-(P_{680}^+) and Q_A^-. Stabilization of Tyr-Z^+(P_{680}^+) in the UV-B-irradiated cells is most likely the consequence of impaired electron transfer from the Mn cluster. Thus, our results provide evidence for the inactivation of the water-oxidizing complex by UV-B light in intact cells in the same way that was observed in isolated preparations (*7*).

The relationship between donor- and acceptor-side damage in UV-B-irradiated PSII is an important issue. A number of previous observations indicate that modifications of the PSII donor side can alter the redox characteristics of acceptor-side components (*40*, *41*). Thus, UV-B-induced impairment of the water-oxidizing complex may trigger the modification of the Q_B binding niche. On the other hand, the observation of modified inhibitor binding in oxygen-eevolving centers shows that the Q_B pocket can be altered in UV-B-irradiated centers, which retain a functional water-oxidizing complex. On the basis of the data presented here, we prefer a model in which the Q_B binding niche may be modified by UV-B radiation prior to inactivation of the water-oxidizing complex,

but oxygen evolution is lost due to the impairment of electron transfer between the catalytic Mn cluster and the reaction center.

Interaction of White Light with the UV-B Effect. Under natural conditions, some UV-B light is always accompanied by the visible part of the solar spectrum. Thus, it is very important to understand the interplay between the effects of the two spectral ranges. Previous results have indicated a synergistic enhancement in the turnover rate of the D1, and also of the D2 reaction center protein, which provides the binding site for Q_A, under a mixture of low-intensity UV-B and visible light (*19*). This effect was interpreted as an indication of enhanced UV damage of PSII mediated by Q_A^- which is formed by illumination with white light. Other studies, however, have shown a protective effect of strong white light (*42*).

Illumination of *Synechocystis* cells with UV-B light induces only a small extent of Q_A reduction in the absence of DCMU. However, a considerable degree of Q_A reduction occurs in the presence of DCMU (in 60% of the centers). Importantly, despite the large difference in the amount of reduced Q_A, the extent of PSII damage is the same when UV-B illumination is applied alone or in combination with DCMU. This finding demonstrates that Q_A^- is unlikely to be a specific mediator of UV-B-induced damage of PSII.

Illumination of the cells with white light at an intensity similar to that used during growth provides clear protection against UV damage as revealed by the slower loss of total fluorescence amplitude and slower induction of fast Q_A^- recombination with Tyr-Z^+(P_{680}^+) (Figure 5), as well as by the slower inhibition of oxygen evolution (Figure 6). The complete cancellation of this beneficial effect by the protein synthesis inhibitor lincomycin (Figure 6) demonstrates that white light decreases the extent of UV-B damage by facilitating de novo synthesis of the D1 and D2 reaction center proteins, which is required for PSII repair. The protection by white light against UV-B-induced damage is an important observation. Our previous results showed a strong induction of the *psbA* and *psbD* genes, encoding the D1 and D2 proteins, respectively, by low-intensity UV-B light (*25*, *43*). This UV-B-induced transcription of the *psbA* and *psbD* genes is not affected by background illumination with white light with an intensity similar to that applied here. Consequently, the facilitation of PSII repair by white light probably occurs at the level of translation, or during the process of PSII assembly and reactivation.

The in vivo characterization of the effect of low-intensity UV-B light on PSII function described in this paper demonstrates that electron transfer from the Mn cluster to Tyr-Z and the reaction center is impaired in intact cyanobacterium cells. The donor-side damage is accompanied by a modification of the Q_B pocket, which affects the binding of plastoquinone and electron transport inhibitors. These findings support the validity of earlier results obtained with isolated PSII preparations at much higher UV-B levels, and exclude the possibility of artifacts due to unphysiological conditions.

REFERENCES

1. Bornman, J. F. (1989) *J. Photochem. Photobiol., B 4*, 145−158.
2. Vass, I. (1996) in *Handbook of Photosynthesis* (Pessarakli, M., Ed.) pp 931−950, Marcel Dekker, Inc., New York.
3. Andersson, B., and Styring, S. (1991) *Curr. Top. Bioenerg. 16*, 1−81.
4. Nanba, O., and Satoh, K. (1987) *Proc. Natl. Acad. Sci. U.S.A. 84*, 109−112.
5. Renger, G., Völker, M., Eckert, H. J., Fromme, R., Hohm-Veit, S., and Graber, P. (1989) *Photochem. Photobiol. 49*, 97−105.
6. Hideg, É., Sass, L., Barbato, R., and Vass, I. (1993) *Photosynth. Res. 38*, 455−462.
7. Vass, I., Sass, L., Spetea, C., Bakou, A., Ghanotakis, D., and Petrouleas, V. (1996) *Biochemistry 35*, 8964−8973.
8. Post, A., Lukins, P. B., Walker, P. J., and Larkum, A. W. D. (1996) *Photosynth. Res. 49*, 21−27.
9. Greenberg, B. M., Gaba, V., Canaani, O., Malkin, S., Mattoo, A. K., and Edelman, M. (1989) *Proc. Natl. Acad. Sci. U.S.A. 86*, 6617−6620.
10. Melis, A., Nemson, J. A., and Harrison, M. A. (1992) *Biochim. Biophys. Acta 1100*, 312−320.
11. Jansen, M. A. K., Greenberg, B. M., Edelman, M., Mattoo, A. K., and Gaba, V. (1996) *Photochem. Photobiol. 63*, 814−817.
12. Yerkes, C. T., Kramer, D. M., Fenton, J. M., and Crofts, A. R. (1990) in *Current Research in Photosynthesis* (Baltscheffsky, M., Ed.) Vol. II, pp 6.381−6.384, Kluwer Academic Publishers, Dordrecht, The Netherlands.
13. Trebst, A., and Depka, B. (1990) *Z. Naturforsch. 45c*, 765−771.
14. Friso, G., Spetea, C., Giacometti, G. M., Vass, I., and Barbato, R. (1993) *Biochim. Biophys. Acta 1184*, 78−84.
15. Friso, G., Barbato, R., Giacometti, G. M., and Barber, J. (1994) *FEBS Lett. 339*, 217−221.
16. Barbato, R., Frizzo, A., Friso, G., Rigoni, F., and Giacometti, G. M. (1995) *Eur. J. Biochem. 227*, 723−729.
17. Tandori, J., Máté, Z., Vass, I., and Maróti, P. (1996) *Photosynth. Res. 50*, 171−179.
18. Bornman, J. F., Björn, L. O., and Akerlund, H.-E. (1984) *Photobiochem. Photobiophys. 8*, 305−313.
19. Jansen, M. A. K., Gaba, V., Greenberg, B. M., Mattoo, A. K., and Edelman, M. (1996) *Plant J. 9*, 693−699.
20. Jansen, M. A. K., Gaba, V., and Greenberg, B. M. (1998) *Trends Plant Sci. 3*, 131−135.
21. Crofts, A. R., and Wraight, C. A. (1983) *Biochim. Biophys. Acta 726*, 149−185.
22. Vass, I., Styring, S., Hundal, T., Koivuniemi, A., Aro, E.-M., and Andersson, B. (1992) *Proc. Natl. Acad. Sci. U.S.A. 89*, 1408−1412.
23. Trtilek, M., Kramer, D. M., and Koblizek, M. (1997) *J. Lumin. 72*−*74*, 597−599.
24. Herdmann, M., Deloney, S. F., and Carr, N. G. (1973) *J. Gen. Microbiol. 79*, 233−237.
25. Máté, Z., Sass, L., Szekeres, M., Vass, I., and Nagy, F. (1998) *J. Biol. Chem. 273*, 17439−17444.
26. Rontó, Gy., Fekete, A., Gáspár, S., and Módos, K. (1989) *J. Photochem. Photobiol., B 3*, 497−507.
27. Diner, B. A. (1998) Photosynthesis: Molecular Biology of Energy Capture; in *Methods in Enzymology* (McIntosh, L., Ed.) Vol. 297, pp 337−360, Academic Press, San Diego, CA.
28. Bennoun, P. (1994) *Biochim. Biophys. Acta 1186*, 59−66.
29. Cheniae, G. M., and Martin, I. (1971) *Plant Physiol. 47*, 568−575.
30. Bennoun, P. (1970) *Biochim. Biophys. Acta 216*, 357−363.
31. Campbell, D., Hurry, V., Clarke, A. K., Gustafsson, P., and Öquist, G. (1998) *Microbiol. Mol. Biol. Rev. 62*, 667−683.
32. Sass, L., Spetea, C., Máté, Z., Nagy, F., and Vass, I. (1997) *Photosynth. Res. 54*, 55−62.
33. Masi, A., and Melis, A. (1997) *Biochim. Biophys. Acta 1321*, 183−193.
34. Shopes, R. J., and Wraight, C. A. (1985) *Biochim. Biophys. Acta 806*, 348−356.
35. Robinson, H. H., and Crofts, A. (1983) *FEBS Lett. 153*, 221−226.

36. Demeter, S., Vass, I., Hideg, É., and Sallai, A. (1985) *Biochim. Biophys. Acta 806*, 16−27.
37. Renger, G., Voss, M., Graber, P., and Schulze, A. (1986) in *Stratospheric Ozone Reduction, Solar Ultraviolet Radiation and Plant Life* (Worrest, C., and Caldwell, M. M., Eds.) pp 171−184, Springer, Berlin.
38. Chu, H.-A., Nguyen, A. P., and Debus, R. J. (1994) *Biochemistry 33*, 6137−6149.
39. Metz, J. G., Nixon, P. J., Rogner, M., Brudvig, G. W., and Diner, B. A. (1989) *Biochemistry 28*, 6960−6969.
40. Krieger, A., and Weis, E. (1992) *Photosynthetica 27*, 89−98.
41. Krieger, A., Weis, E., and Demeter, S. (1993) *Biochim. Biophys. Acta 1144*, 411−418.
42. Bornman, J. F., and Teramura, A. H. (1993) in *Environmental UV Photobiology* (Young, A. R., Björn, L. O., Moan, J., and Nultsch, W., Eds.) pp 427−479, Plenum Press, New York and London.
43. Vass, I., Máté, Z., Sass, L., Viczián, A., Nagy, F., Kirilovsky, D., and Etienne, A.-L. (1999) in *Photosynthesis: Mechanisms and Effects* (Garab, Gy., Ed.) pp 2109−2114, Kluwer Academic Publishers, Dordrecht, The Netherlands.
44. Lavorel, J., Lavergne, J., and Etienne, A.-L. (1982) *Photobiochem. Photobiophys. 3*, 287−314.

BI991094W